Journal of Hydrometeorology (Proof Only)

Are General Circulation Models Ready for Operational Streamflow Forecasting for Water Management in the Ganges and Brahmaputra River Basins?

SAFAT SIKDER, XIAODONG CHEN, AND FAISAL HOSSAIN

Department of Civil and Environmental Engineering, University of Washington, Seattle, Washington

JASON B. ROBERTS AND FRANKLIN ROBERTSON

National Space Science Technology Center, NASA Marshall Space Flight Center, University of Alabama in Huntsville, Huntsville, Alabama

C. K. SHUM

Division of Geodetic Science, School of Earth Sciences, The Ohio State University, Columbus, Ohio, and Institute of Geodesy and Geophysics, Chinese Academy of Sciences, Wuhan, China

FRANCIS J. TURK

Jet Propulsion Laboratory, California Institute of Technology, Pasadena, California

ABSTRACT

This study asks the question of whether GCMs are ready to be operationalized for streamflow forecasting in South Asian river basins, and if so, at what temporal scales and for which water management decisions are they likely to be relevant? The authors focused on the Ganges, Brahmaputra, and Meghna basins for which there is a gridded hydrologic model calibrated for the 2002–10 period. The North American Multimodel Ensemble (NMME) suite of eight GCM hindcasts was applied to generate precipitation forecasts for each month of the 1982–2012 (30 year) period at up to 6 months of lead time, which were then downscaled according to the bias-corrected statistical downscaling (BCSD) procedure to daily time steps. A global retrospective forcing dataset was used for this downscaling procedure. The study clearly revealed that a regionally consistent forcing for BCSD, which is currently unavailable for the region, is one of the primary conditions to realize reasonable skill in streamflow forecasting. In terms of relative RMSE (normalized by reference flow obtained from the global retrospective forcings used in downscaling), streamflow forecast uncertainty (RMSE) was found to be 38%–50% at monthly scale and 22%–35% at seasonal (3 monthly) scale. The Ganges River (regulated) experienced higher uncertainty than the Brahmaputra River (unregulated). In terms of anomaly correlation coefficient (ACC), the streamflow forecasting at seasonal (3 monthly) scale was found to have less uncertainty (>0.3) than at monthly scale (<0.25). The forecast skill in the Brahmaputra basin showed more improvement when the time horizon was aggregated from monthly to seasonal than the Ganges basin. Finally, the skill assessment for the individual seasons revealed that the flow forecasting using NMME data had less uncertainty during monsoon season (July–September) in the Brahmaputra basin and in postmonsoon season (October–December) in the Ganges basin. Overall, the study indicated that GCMs can have value for management decisions only at seasonal or annual water balance applications at best if appropriate historical forcings are used in downscaling. The take-home message of this study is that GCMs are not yet ready for prime-time operationalization for a wide variety of multiscale water management decisions for the Ganges and Brahmaputra River basins.

Corresponding author address: Dr. Faisal Hossain, Department of Civil and Environmental Engineering, University of Washington, 201 More Hall, Box 352700, Seattle, WA 98195.
E-mail: fhossain@uw.edu

1. Introduction

General circulation models (GCMs) are most commonly applied as tools for making long-term ($\sim$50–100 years) projections on future climate based on natural

TABLE 1. Summary of water resources vulnerability indicators for South Asian nations.

Country	Population density (km^{-2})	GDP per capita/HDI[a]	Water vulnerability index[a]	Major issues of water vulnerability[b]
Bangladesh	1060	$406/137	0.45	FL, DR, CYC, GW CONT, and GLM
Pakistan	202	$632/134	0.60	FL, DR, and CYC
India	334	$640/126	0.50	FL, DR, CYC, GLM, and GW CONT
Nepal	179	$252/138	0.40	GLB and GLM
Afghanistan	40	$202/—	0.60	DR and GLM
Myanmar	74	$702/132	0.30	FL and CYC
Vietnam	259	$1170/113	0.31	FL and GW CONT

[a] Statistics derived from UNEP (2008) report. HDI is the Human Development Index rank (out of all nations).
[b] FL, flood; DR, drought; CYC, cyclone; GW CONT, groundwater contamination (arsenic); GLM, glacier melt; and GLB, glacier burst. Water vulnerability is derived by UNEP (2008) and varies from 0 to 1, with 1 being highly vulnerable water resources.

and anthropogenic scenarios (IPCC 2013). At the heart of their projection-making ability lies a four-dimensional framework (x, y, z, and t) to model the land, ocean, and atmosphere processes of the entire Earth in a coupled manner. This requires a comprehensive computational platform to model the physics, albeit with certain parameterizations, to achieve realistic solutions of the future state of Earth's climate. Historically, GCMs have been used mostly for addressing climate issues (Wilby et al. 1998; Yuan et al. 2015) in the framework of a boundary value problem (Pielke 1998). There is now an ongoing discussion if such models, with proper initialization, especially for the ocean and land states, can also be used to operationally forecast future climate variability at seasonal to interannual time scales (Kundzewicz and Stakhiv 2010; Salas et al. 2012). For example, to predict streamflow at monthly to seasonal scales using a hydrologic model, GCMs can potentially provide vital information about the soil condition to initialize the model as well as the atmospheric boundary to force the model (Yuan et al. 2015).

South Asia represents a clear case where such short-term climate forecasts (of mostly precipitation) could play a vital role in the water management and planning decisions for water agencies. More than 700 million people of South Asian nations, comprising India, Pakistan, Nepal, Bhutan, Bangladesh, Myanmar, Thailand, Cambodia, and Vietnam, depend on the climate-sensitive Himalayan glaciers for a significant supply of water (Table 1). There are several societal issues that make the operational use of seasonal-scale precipitation forecast from GCMs urgent for this populous region. First, year-round cropping to support the green revolution and food demand of South Asian nations means that the agricultural lands are never left fallow with three major growing seasons (e.g., spring–summer, summer–fall, and winter–spring). Consequently, these agricultural lands not only depend on the monsoon rains

during the summer–fall (May–October) growing seasons, but they also heavily depend on the glacier- and snow-fed groundwater (deep and shallow) during the nonmonsoon growing seasons when streamflow or surface water availability is either low or receding (Byerlee 1992). Second, South Asia is vulnerable to uncoordinated human activity in the upstream (higher elevation) regions, such as extraction, diversion, and dam impoundment of river waters. Some pertinent examples are the Farakka Barrage (on the Ganges River; Mirza 1998), the Gozaldoba Barrage (on the Teesta River, a tributary of the Brahmaputra; Nishat and Faisal 2000), the now-shelved Tipaimukh Dam on the Meghna River in India (Sinha 1995), and the much-discussed Indian River Linking Project (IRLP; Misra et al. 2007). This anthropogenic variability due to the artificial redistribution of water (with no coordination with downstream water planning agencies) is compounded further by the seasonal variability of flow due to the monsoon. Overall, the coevolving human and natural drivers present a challenge for water managers, particularly those tasked with water resources planning and improving irrigation practices at seasonal or interseasonal time scales. Thus, forecasting surface water availability can be useful for making proactive decisions on water management (Hossain et al. 2013).

To grasp the need for forecast of water availability along with a clear understanding of regional-scale human impacts, consider the case of the Institute of Water Modeling (IWM) in Bangladesh. The IWM functions as a trust organization for the Government of Bangladesh and is the main technical partner for water-related decision-making activity for the Ministry of Water Resources of Bangladesh (see Hossain et al. 2014). One of the pressing needs for the IWM is to provide guidance to farmers who operate low-lift pumps for groundwater extraction (during December–April) and those who depend on surface water irrigation schemes in the Ganges tributaries (during October–December). A key

AU19
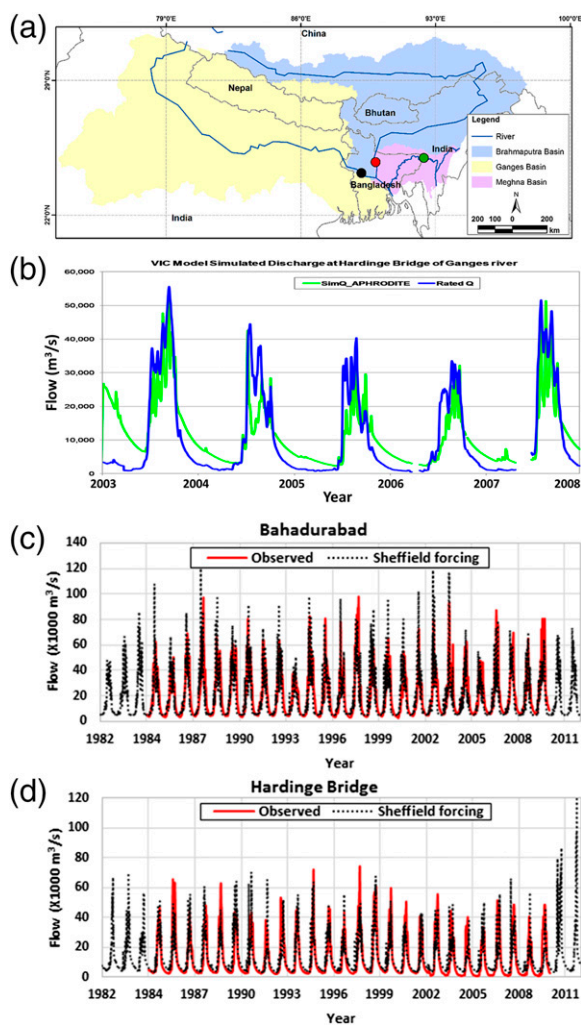
FIG. 1 . (a) The GBM basins that are currently modeled by VIC-3L to simulate surface runoff streamflow. ~~The triangles are water planning units that were randomly selected to assess the skill of GCM forecast precipitation-based projection of water availability.~~ The solid circles represent streamflow locations at the Ganges (black), Brahmaputra (red), and Meghna (green) rivers. (b) Discharge simulation by VIC-3L using in situ and gridded forcing (green line) and observed (blue line) data at the Ganges River [Hardinge Bridge location, black circle in (a); after Siddique-E-Akbor et al. (2014)]. (c) Streamflow simulated by the Sheffield data for the Brahmaputra River at Bahadurabad for 1982–2012. (d) As in (c), but for Ganges River at Hardinge Bridge location. Note that performance metrics are shown in Table 3.

surface water irrigation scheme in Bangladesh is based on one of the major tributaries of the Ganges River (known as Gorai) as it enters Bangladesh in the northwest (Fig. 1a). On the other hand, most groundwater-based irrigation occurs in the Brahmaputra basin (which is mostly unregulated) in the northern part of Bangladesh (Fig. 1a). In both cases, skillful forecast of surface water availability is needed a few months ahead. For the

F1 AU4

AU5

Ganges River, Indian stakeholder agencies in the upstream begin extensive diversion and withdrawal of flow during the nonmonsoon period, which causes the downstream flow hydrograph to rapidly recede at downstream locations in Bangladesh. The converse is true for Brahmaputra River, which is a fast-flowing and rain-fed river basin. Thus, any precipitation forecast–based projection of water availability via hydrologic modeling can be directly useful for season-to-season irrigation planning in Bangladesh if there is skill in the forecast. However, a hydrologic model without an upstream regulation component may not be able to pick up the human-altered recession in the downstream location, and thus, simple bias adjustment of recession flow (i.e., subtracting or adding to flow approximately the flux that is being withdrawn in the upstream) during the nonmonsoon period may be required to make the most of precipitation forecasts. This is in fact a common practice used by water managers.

A few other agencies in the region that have very similar decision-making needs are the Indus River System Authority (IRSA) in Pakistan, which provides guidance on the operation of water regulation structures of Indus basin, and the Central Water Commission (CWC) in India. Operational agencies are now aware that the stand-alone use of physics-based numerical models (e.g., GCMs and hydrologic and hydraulic models) that mimic the physical laws of nature may not be sufficient to project water availability that is now increasingly dominated by human decisions made by competing users and nations (see, e.g., Vogel 2011; Hossain 2013). However, forecasts of surface water availability from numerical models remains an objective, physically based starting point for an agency to add a water management component based on proxy information on how the water is likely to be regulated by the competing user located in the upstream (transboundary) region.

AU6

Based on the above tenet, this study investigates the question of whether GCMs are ready to be operationalized for streamflow forecasting for water management in South Asian river basins, and if so, at what temporal scales and water management decisions are they likely to be relevant? GCMs are essentially tailored for top-down and global-to-regional assessments and decision-making (Wilby et al. 1998). Water management decisions by agencies at seasonal time scales are typically made at smaller spatial scales than the scale at which GCMs are generally applied. GCM-idealized physics processes (parameterizations) are designed for function at the computational scales on the order of 100 km and are tuned to produce realistic and energetically consistent large-scale climate. Thus, there are significant

uncertainties in scaling issues and the degree to which these parameterizations can deliver realistic means and distributions of hydrometeorological variables at their finest scales relevant for decision-making. At issue is how effectively these quantities can be downscaled to drive applications (e.g., hydrologic or agricultural) models whose processes operate at much finer scales. Before GCMs can be operationally implemented for short-term (seasonal scale) decision-making for water management by South Asian agencies, a rigorous assessment of the skill of GCM is essential. End-users are particularly interested in performance metrics, including uncertainties, when evaluating whether to operationalize any new forecast product on the fly.

It should be noted that the development of streamflow forecasting systems for South Asia and in other regions has been ongoing for a number of years given the frequent occurrence of large-scale flooding and drought problems (i.e., first in the Ganges and Brahmaputra basins in Bangladesh and more recently in the Indus basin in Pakistan). Many of these systems typically have a flood-centric focus and not necessarily a water management-centric objective. For example, Shrestha et al. (2014) have demonstrated the forecasting of daily mean streamflow at an unregulated river location in the upper Indus using numerical weather prediction initial states from the European Centre for Medium-Range Weather Forecasts (ECMWF) to drive a hydrologic model. Webster (2013) has called for a need to improve weather forecasts in the developing world. Hopson and Webster (2010) have developed an automated system for streamflow forecasting in Bangladesh at 1–10 days by propagating calibrated ECMWF precipitation forecast ensembles through a hydrologic model. The platform for such a system was provided by Jian et al. (2009) who explored the large-scale controls on streamflow at intraseasonal time scales. For gaining an understanding of the rich heritage of using climate signals in extending forecasts of hydrologic prediction systems in the United States, the reader is referred to the review of literature provided in Hamlet and Lettenmaier (1999a,b) and Wood et al. (2002). More recently, Yuan et al. (2015) have reviewed t~~he state of the art on~~ current climate model–based hydrologic forecasting.

Given the dominance of a monsoonal system where the majority of the precipitation occurs over a 3–5-month period, the surface water availability (flow in major rivers) is highly seasonal and skewed. At major river locations in downstream regions, such as Hardinge Bridge on the Ganges River or Bahadurabad on the Brahmaputra River (Fig. 1a there exists multidecadal records of streamflow (spanning at least 30 years or more). Such records allow the construction of flow climatology that is already used for decision-making by water management agencies at seasonal to annual time scales. Although GCMs are typically optimized to produce climate forecasts and not weather forecasts, it is nevertheless worthwhile to assess the value added by GCM-based streamflow forecasting beyond the traditional use of flow climatology.

In this study, we focus exclusively on the Ganges, Brahmaputra, and Meghna (GBM) river basins for which we have a comprehensive and calibrated hydrologic model, the three-layer Variable Infiltration Capacity model (VIC-3L; Liang et al. 1994). This model was used to convert the hydrometeorological (climate) forecast (of precipitation, temperature, and wind speed) into forecasts of surface water availability, primarily streamflow. In the remaining sections, we provide a brief overview of the North American Multimodel Ensemble (NMME) experiment protocol (Kirtman et al. 2014). This is followed by a discussion of the study region and an overview of the streamflow predictability using VIC-3L to accurately capture streamflow dynamics. A discussion of the necessary skill corrections and downscaling of the seasonal forecasts follows. Finally, we present our findings on the forecast skill of precipitation and streamflow to evaluate how ready GCMs are for prime-time use by South Asian agencies. We openly discuss the key issues that need a resolution to raise the application readiness of GCM-based forecasting of water availability for water managers of South Asia. This study presents an application-oriented investigation aimed at judging the application readiness level (ARL) of GCMs for seasonal-scale transboundary water management in South Asia.

2. NMME for precipitation forecasting

We have applied the suite of general circulation models that have recently been organized under the auspices of the NMME initiative. As advocated by a recent U.S. National Academies report (NRC 2010), a collaborative and coordinated implementation strategy for the NMME prediction system is currently delivering real-time, global, seasonal-to-interannual predictions on the NOAA Climate Prediction Center (CPC) operational schedule (Kirtman et al. 2014). It is expected that multimodel ensembles provide improved forecasts through not only systematic error cancellation but improved sampling of the true forecast distribution (Hagedorn et al. 2005).

The NMME protocol consists of 9-month lead (at minimum) dynamical forecasts from nine participating GCMs. A detailed list of experimental setup, available models, number of ensembles, and hindcast period can

AU7
AU8
AU9

TABLE 2. List of NMMEs utilized in this study.

Model	Hindcast period	Ensemble size	Max lead (months)	Version
Canadian Coupled Global Climate Model	1981–2010	10	11.5	Fourth Generation (CanCM4)
Community Climate System Model	1982–2010	6	11.5	3 (CCSM3)
	1982–2010	10	11.5	4 (CCSM4)
Geophysical Fluid Dynamics Laboratory Climate Model	1982–2010	10	11.5	2.1 (GFDL CM2.1)
	1981–2010	12	11.5	2.5 (GFDL CM2.5_FLOR-A06)
	1981–2010	12	11.5	2.5 (GFDL CM2.5_FLOR-B01)
Goddard Earth Observing System Model	1981–2010	12	8.5	5 (GEOS-5)
Climate Forecast System	1982–2010	24	9.5	2 (CFSv2)

T2 be found in Kirtman et al. (2014). Here, Table 2 provides an adapted (from Kirtman et al. 2014) and updated list of the models that are currently (as of March 2015) providing real-time forecasts and are used for constructing the multimodel ensemble forecasts. Briefly, both real-time forecasts and a set of hindcasts generally covering the period 1981–2010 are available through the International Research Institute (IRI) for Climate and Society data portal. Archived forecast variables include precipitation, sea surface temperature (SST), and 2-m air temperature. As the NMME progresses during its second phase, a more expansive set of archived variables is being made available (Kirtman et al. 2014). Thus, the choice of NMME for our skill assessment was deemed appropriate given the increasing versatility (beyond just a few hydrometeorological variables) that NMME is expected to afford in the upcoming years. The total multimodel ensemble utilized in this study consists of 96 members obtained from eight of the contributing models. In section 5, we discuss the treatment of NMME-forecasted hydrometeorological variables for the development of downscaled scenarios necessary for resolving surface water availability at hydrologically relevant scales.

3. Study region

The study region is the GBM basin of South Asia. The total catchment area of the GBM basin is about 1.72×10^6 km². The countries within the GBM basin are Bangladesh, India, Nepal, Bhutan, and China. The geographical location of the GBM basin is between 21° and 31°N and 73° and 97°E. The Ganges, Brahmaputra, and Meghna Rivers are the three major rivers in the GBM basin. The Himalayan and Vindhya ranges are the sources of these three rivers (Nishat and Rahman 2009). The catchment areas of different countries within the GBM basin are furnished in Table 3 (http://www.jrcb.gov.bd/). A map showing the region is in Fig. 1a.

The GBM basin exhibits extremes in surface water availability. Annual rainfall in the GBM ranges from 990 to 11 500 mm (Shah 2001). Streamflow in the downstream regions of the Brahmaputra and Ganges Rivers can vary from 5000 in winter to 80 000 m³ s⁻¹ during the monsoon season (Mirza 1998). The Himalayan Range covers about 15 000 glaciers, which store about 12 000 km³ of freshwater (Dyurgerov and Meier 2005). Thus, annual water distribution in the GBM basin is highly dominated by the storage of precipitation over a long period in the Himalayas (Chowdhury and Ward 2004). In contrast, the Vindhya Range in the south, at elevations spanning 450–1100 m, contributes significant amounts of orographic precipitation to nourish the southern tributaries of the Ganges–Yamuna system. The GBM river system is the third-largest (behind the Amazon and Congo) freshwater outlet to the world's oceans (Chowdhury and Ward 2004).

4. VIC-3L

The Variable Infiltration Capacity model, first developed by Liang et al. (1994), was used as the macroscale distributed hydrological model. VIC is a large-scale, semidistributed macroscale hydrological model. It is capable of solving full water and energy balances. The minimum set of input forcing data that are required for simulation of the hydrologic fluxes is 1) precipitation, 2) temperature

TABLE 3. Geographic and hydrologic model properties of the GBM basins.

River basin	Area (km²)	Model gridcell resolution (km)	Number of grids	Peak elev (m)
Ganges	1 087 300	12.5	5506	3892
Brahmaputra	552 000	25.0	1550	8848
Meghna	82 000	12.5	1171	600

TABLE 4. Performance of VIC-3L during 2002–10 using in situ gridded and SGF data (shown in parentheses). Performance metrics are shown for streamflow simulation against observed measurements at two downstream locations of GBM basins shown in Fig. 1.

Basin	Season	RMSE ($m^3\,s^{-1}$)	Correlation	Efficiency
Brahmaputra location: Bahadurabad	Dry (Nov–May)	7847 (7340)	0.74 (0.73)	0.45 (0.39)
	Wet (Jun–Oct)	16 230 (14 615)	0.84 (0.75)	0.70 (0.40)
	Full year	12 088 (11 013)	0.92 (0.88)	0.83 (0.75)
Ganges location: Hardinge Bridge	Dry (Nov–May)	4510 (4045)	0.86 (0.85)	0.23 (0.54)
	Wet (Jun–Oct)	10 733 (12 931)	0.80 (0.54)	0.46 (0.25)
	Full year	7750 (8919)	0.88 (0.75)	0.73 (0.55)

(minimum and maximum), and 3) wind speed. The basic features of VIC are as follows:

1) The land surface is modeled as a (lumped) grid of large (e.g., 12.5 km), flat, uniform cells.
2) Inputs to the model are time series of daily or subdaily meteorological drivers (e.g., rainfall, snow, air temperature, and wind speed).
3) Land–atmosphere fluxes, and the water and energy balances at the land surface, are simulated at a daily or subdaily time step. Water can only enter a grid cell via the atmosphere.
4) Grid cells are simulated independently of each other, and the entire simulation is run for each grid cell separately, one grid cell at a time, rather than for each time step, looping over all grid cells.
5) Routing of streamflow is performed separately from the land surface simulation, using a separate model. In this study, we used the routing model of Lohmann et al. (1998).

Previous applications of VIC in nearby and similar environments are reported in the work of Costa-Cabral et al. (2008) for the Mekong basin, Shrestha et al. (2014) for the Indus basin, and Wu et al. (2012) for the South Asian region. Flow routing was carried out at the locations of streamflow gauging (at Bahadurabad station in the Brahmaputra River and Hardinge Bridge in the Ganges River). The streamflow simulation using in situ forcing data (gridded from in situ weather station measurements that were available only from 2002 to 2010) is shown in Fig. 1b along with in situ (i.e., observed) flow measurements. Table 4 provides a summary of the performance of the calibrated VIC-3L against streamflow observations. On the other hand, the in situ flow-calibrated VIC-3L could be applied over a much longer period (30 years) because of availability of long-term retrospective global forcings archived by Sheffield et al. (2006, 2012) that were used for downscaling of GCM forecast forcings. Hydrologic simulation from 1982 to 2012 was therefore used in the skill assessment of flow forecasting relative to the retrospective global forcing. For further details on the calibration, validation, and in situ dataset preparation, the reader is referred to Siddique-E-Akbor et al. (2014).

Given the hydrological characteristics of the GBM basin dominated by a strong monsoonal signal each year (during June–September), streamflow in large rivers shows well-defined seasonality, particularly at lower regions of the basin with higher drainage area. Figures 1c and 1d show the simulation of streamflow for the Ganges River using in situ records that the water resources and planning division of IWM in Bangladesh already use for seasonal-scale decision-making on water management. It should be kept in mind that this conventional decision-making on water management for the whole region of Bangladesh is afforded only at few locations where a continuous record of flow gauging exists since the 1960s for building and updating flow climatology. Thus, a spatially distributed model, if it is demonstrated to have skill at these select locations, can be a platform for estimating forecast climatology at ungauged locations (or at a collection of grid cells) where there is no measurement and yet water management decisions need to be made based on mean annual or seasonal flow or flow duration curves.

Our VIC-3L simulation of streamflow using the 1982–2012 retrospective global forcing of Sheffield et al. (2006), which is used as the baseline for downscaling GCM outputs, indicates that the VIC-simulated streamflow captures quite well the interannual and interseasonal variability (for 17 out of 26 years where in situ flow data were available from 1985 to 2010; Figs. 1c,d). The performance metrics of VIC-3L using this baseline forcing is comparable to those obtained with in situ forcing data for the same study period (see Table 4 and Figs. 1c,d). The long-term anomaly (Figs. 2a,b) of the simulated streamflow from global forcing (Sheffield et al. 2006) indicated that the reference forcing (used for downscaling of GCM forecast forcing) can capture the interannual variability for most years. For example, both basins were able to capture the extreme flooding events of 1988 and 1998 in lower regions of the Ganges and Brahmaputra basins. The annual anomaly of the Brahmaputra basin from Sheffield global forcing (SGF) matched well qualitatively (as a trend) with the observed anomaly up to 1998 and again during 2004–09 (Fig. 2a). For Ganges at Hardinge
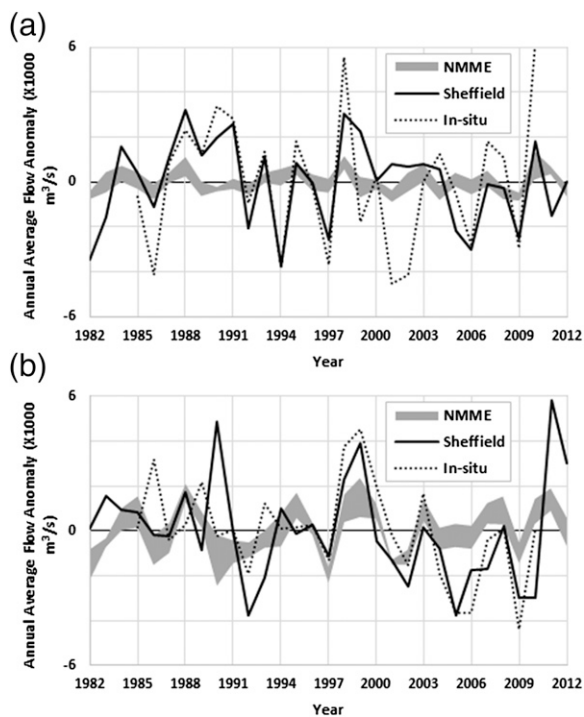
FIG. 2. (a) Annual average anomaly of in situ observed flow, outflow simulated using the SGF data, and outflow from six different lead times of average NMME at Bahadurabad in the Brahmaputra River. (b) As in (a), but for Hardinge Bridge in the Ganges River.

Bridge location, the SGF yielded better agreement in picking up observed flow anomaly after 1994, which is an intriguing but unverifiable coincidence as the Ganges water sharing treaty between the governments of India and Bangladesh was signed in 1996 (Fig. 2b).

In general, we observe that the accuracy of the simulated flow during the 1982–2012 time period using the retrospective global forcing is significantly reduced (Table 4) as the simulation reflects the uncertainty due to both VIC and the SGF dataset. If we assume that VIC is able to perfectly represent the rainfall–runoff process of the basins, the quality of the simulated streamflow using the global retrospective forcing can be attributed to the uncertainty of the global forcing dataset only (Table 5). Comparing the values reported in Table 4 with those shown in Table 5 indicates that high uncertainty is introduced into the simulated flow because of uncertainty in the retrospective global forcing data. As an initial proof-of-concept study to assess prime-time readiness of GCM for operational streamflow forecasts, we circumvented this problem by treating the streamflow generated from global forcing–derived flow as reference flow in all subsequent skill assessment. The justification for this is that GCM forecasting forcings will not be able to exceed the skill obtained from the global

forcing used in the downscaling. In this way, the uncertainty involved in the GCM downscaling using the retrospective global forcing of Sheffield et al. (2006) can be avoided to analyze scenarios of what if forcings to downscale GCM were perfect. Nevertheless, in the truest operational sense, we have observed, as will be shown later, that GCM-based streamflow forecasting is not ready for prime time, even for the basic water management applications (such as seasonal to annual water balance decision-making) until the quality of the historical forcing used for downscaling is improved through the creation of a more regionally consistent in situ forcing dataset. In other words, a future study of GCM forecast forcings downscaled on the basis of a more regionally relevant dataset would be worthwhile.

5. Interannual variability and development of downscaled scenarios

Prior to use of the NMME seasonal forecasts, GCM simulations require careful evaluation and must be downscaled to the resolution of the VIC-3L system. GCMs are typically run at a more coarse resolution than numerical weather prediction models. As such, a primary objective of GCMs is to capture the slowly evolving, large-scale components of oceanic and atmospheric dynamics. To understand the relationship between the local-scale GBM rainfall with that at the regional and global scale, an analysis has been performed using the area-average rainfall anomalies.

a. Large-scale relationships

A record of precipitation variability from the Asian Precipitation–Highly-Resolved Observational Data Integration Toward Evaluation of Water Resources (APHRODITE) dataset (Yatagai et al. 2012) has been used to construct a standardized precipitation index (SPI) of GBM area-average rainfall. Global precipitation and SST estimates have been obtained from the Global Precipitation Climatology Project (GPCP; Adler et al. 2003) and the Reynolds et al. (2007) Optimum Interpolation Sea Surface Temperature (OISST) dataset. Figures 3a and 3b are used to illustrate the relationships between the GBM regional-average SPI, rainfall within the GBM itself, and global-scale SST and precipitation. During most months (including January and July as illustrated), the SPI is significantly correlated ($p = 0.10$) with most locations in the GBM region. The remainder of Fig. 3a depicts strong correlations with SST and precipitation throughout the tropics; these patterns are reminiscent of those associated with well-known phenomena such as El Niño–Southern Oscillation (ENSO). It is known that tropical SST variability

TABLE 5. Performance of streamflow using SGF, relative to flow simulated using in situ gridded forcing data (i.e., considering no model uncertainty from VIC-3L during 2002–10). Metrics are shown for 2002–10 to allow for comparison with Table 4 to understand the combined effect of model and input uncertainty.

Basin	Season	RMSE ($m^3\,s^{-1}$)	Correlation	Efficiency
Brahmaputra location: Bahadurabad	Dry (Nov–May)	3523	0.74	0.45
	Wet (Jun–Oct)	13 153	0.76	0.29
	Full year	8926	0.88	0.62
Ganges location: Hardinge Bridge	Dry (Nov–May)	1429	0.88	0.76
	Wet (Jun–Oct)	15 602	0.57	0.33
	Full year	10 156	0.74	0.54

influences atmospheric convection, and together they can influence remote regions through teleconnection patterns (Klein et al. 1999; Alexander et al. 2002). Note that the connection to the GBM regional precipitation anomalies appears stronger for January than July.

It is precisely these large-scale climate anomalies and their remote teleconnections that provide a significant source of seasonal forecasting skill. In Fig. 3b, the same teleconnections are examined between observed SPI interannual variability and forecasted precipitation and sea surface temperature. The correlations are based on the NCEP Climate Forecast System, version 2 (CFSv2), 24-ensemble mean forecast. It is evident that the seasonal climate model forecasts are able to capture similar structures, as observed. However, the amplitudes and locations of the teleconnection patterns can vary systematically from those in Fig. 3a. For example, the model-forecast SST teleconnections are more narrowly constrained along the equator and somewhat eastward. There is also a strong precipitation teleconnection over the northwestern tropical Pacific (near Japan) that is not found in the observations.

b. Raw forecast skill

The inability to fully capture these large-scale relationships has direct influence on the ability of the model to properly translate forcing from remote tropical regions to higher latitudes. The result can be subpar performance of direct model forecasts in these teleconnected regions despite reasonably skillful forecasts within the tropics. While it is possible to apply multivariate corrections (e.g., canonical correlation analysis) trained using the hindcast datasets, it is beyond the scope of this study. Rather, this study will focus on the native forecast skill of the NMME forecasts.

Figure 4 provides an analysis of the probabilistic forecast skill of the raw NMME forecasts. The debiased ranked probability skill score (RPSS) is computed for both rainfall and temperature forecasts following Müller et al. (2005). The RPSS is evaluated at each point within the GBM basin individually, and the area-average RPSS is shown as a function of verifying month and forecast

lead. A positive value of the RPSS indicates the percentage improvement of the NMME forecast of identifying the observed tercile bin—below-, near-, or above-normal monthly average—against that of climatology (i.e., assuming equal chances for each tercile). As shown, only marginal improvement is found on average within the basin against a climatological forecast. The highest, but very modest, skill is found for the shortest lead time. We should note that the evaluation of the RPSS for individual point locations is a very stringent test, as it is expected most skill present is only found at the large, coarse resolution of the GCM. These results indicate a potentially significant shortcoming for providing distributed model forecasts for point locations. Further, it implies that at least some bias correction, particularly one that can improve the probabilistic forecast, may be needed.

c. Bias correction and spatial disaggregation

For application to the VIC-3L, the NMME forecasts must be downscaled to the daily, 0.5° forcing of the model grid. The NMME forecasts are archived at monthly, 1° resolution. As with long-term climate projections, a downscaling approach must be employed. Here, we take the approach of bias correction and spatial disaggregation (CSD), as established in Wood et al. (2002). It is known that coupled general circulation models do not adequately capture the climatological cycle for atmospheric, land, and oceanic variables and require systematic error corrections (Becker et al. 2013). Following Wood et al. (2002), systematic error correction of the monthly forecasts has been implemented through use of a cumulative distribution function (CDF) matching technique. The model distributions of precipitation and temperature are CDF matched to those of the Sheffield et al. (2006) meteorological forcing dataset (SGF) for the years 1982–2012. Gamma distributions are used for the nonzero precipitation estimates while a Gaussian distribution is used for temperature variables. To downscale from the 1° NMME resolution, a local scaling approach is applied to the bias-corrected NMME forecasts. The local scaling factor is equal to the ratio of

AU21
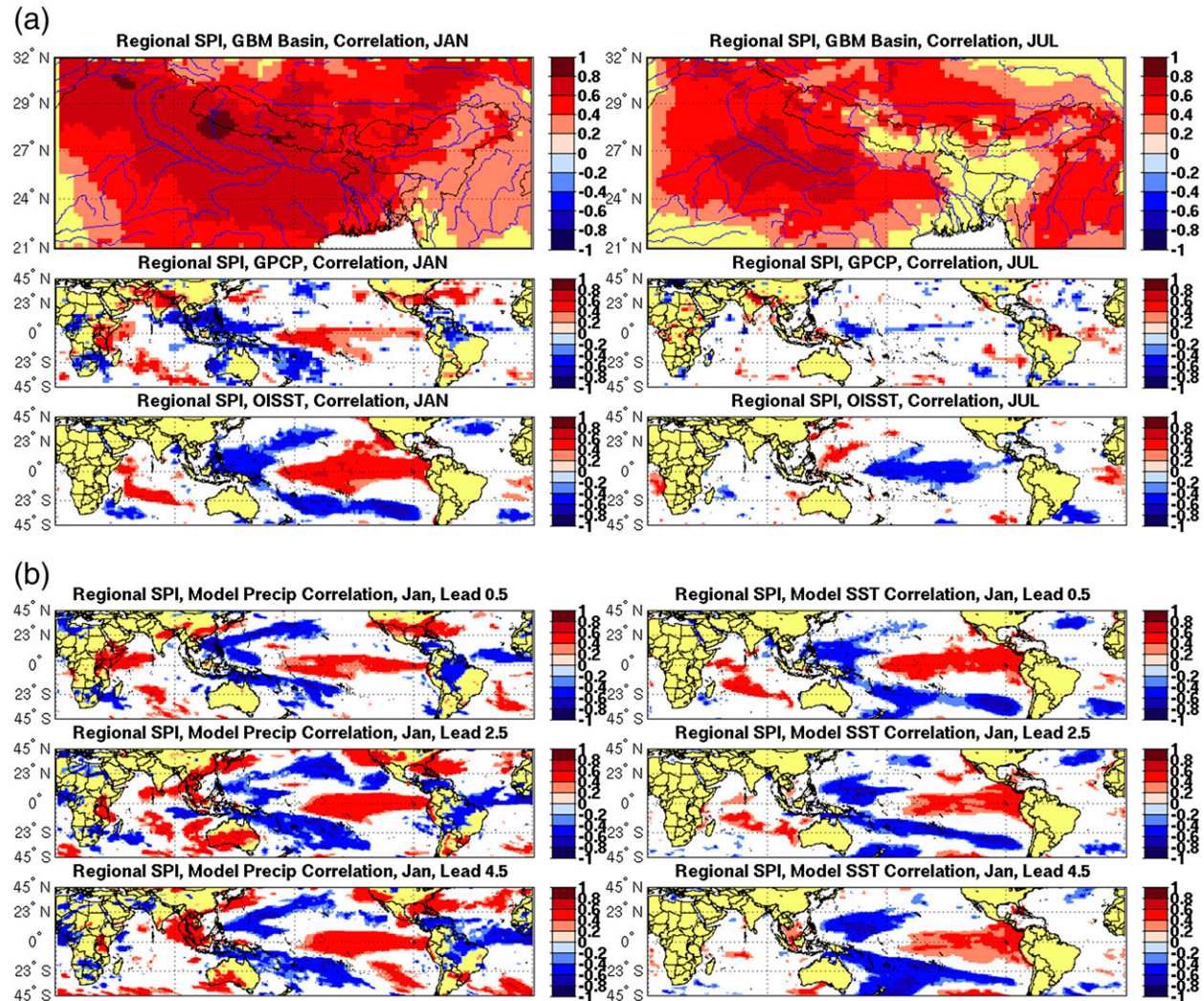
FIG. 3. (a) Observed area-average SPI correlations with observed rainfall (significant at the $p = 0.10$ level) at each point over (top) the GBM basin, with large-scale precipitation from (middle) GPCP and (bottom) SST. Both (left) January and (right) July are illustrated. (b) The observed January area-average SPI correlations with the NMME seasonal forecasts (significant at the $p = 0.10$ level) for (left) precipitation and (right) SST at lead times of (top) 0.5, (middle) 2.5, and (bottom) 4.5 months. Note the similarity of tropical precipitation and SST signals with those in (a).

the climatological high-resolution estimate against that obtained by resampling of the coarse-resolution climatology to the locations of the finer-resolution grid. After correcting monthly mean biases and applying the local scaling factor, daily forcing is obtained by randomly drawing a year (for the appropriate forecast month) from the historical archive of the SGF dataset. The daily values are multiplicatively scaled (zero-bounded quantities) or shifted (nonzero-bounded quantities) to match the bias-corrected NMME forecast at each grid point. If a daily rainfall value results in a value higher than that observed in the historical archive, then its total value is equally spread among its neighboring days. Because only daily average temperature is forecast by NMME,

daily minimum and maximum temperatures were obtained by shifting the SGF average by the same amount, resulting in their average matching the monthly mean, as in Wood et al. (2002). Wind speed is left unadjusted, as the NMME forecasts do not typically provide this variable. The BCSD approach is applied to every forecast lead for every verifying forecast month.

6. Results and discussion

We applied the NMME suite of GCMs as an ensemble of precipitation forecasts that were made for each month of our study period (1982–2012; 372 months) and at up to 6 months of lead time. First, the forecast skill of
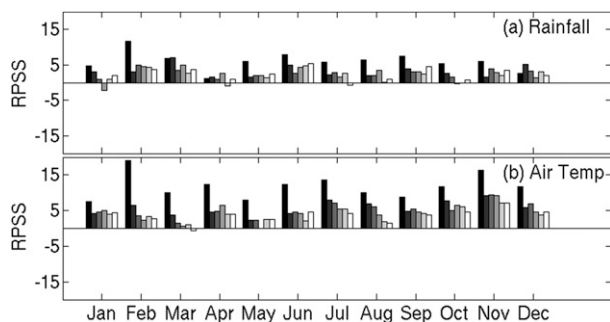
FIG. 4. The GBM area-average RPSS for (a) rainfall and (b) air temperature are shown for all 12 verifying months. Within each grouping by month, the bars indicate the ranked probability skill with increasing forecast lead from 0.5 (black) to 5.5 (white) months (from left to right). The RPSS is computed against the use of climatological tercile (e.g., below, near, and above normal) probabilities.
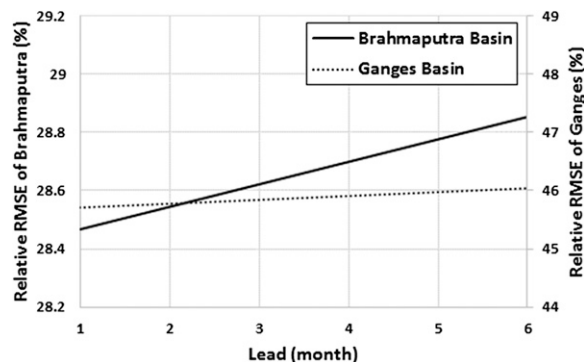
FIG. 5. Relative RMSE (normalized by SGF) trend of NMME precipitation forecast (during 1982–2012) over the entire Ganges and Brahmaputra basin as a function of lead time (months). Note that the trend is idealized as a linear regression mainly to observe sensitivity to lead time.

precipitation data was assessed against the SGF dataset. Here the SGF was used as the reference data for performance analysis, because, as noted earlier, the same dataset was used to downscale the NMME data from monthly to daily scale. As our original input data (NMME data) are in monthly scale, we first show the skill of the forecast at monthly scales. The skill of the NMME precipitation was determined in terms of relative root-mean-square error (RMSE). Also, to quantify the correlation between the observed (SGF) and the NMME forecast, the anomaly correlation coefficient (ACC) was used (Miyakoda et al. 1972). Both matrices were calculated for the entire Ganges and Brahmaputra basins for the time period of 1982–2012.

Figure 5 shows the relative RMSE (normalized by the SGF) trend of the NMME precipitation forecast over the entire Ganges and Brahmaputra basins. It is quite clear that there is no significantly consistent trend of the relative RMSE with lead time. In addition, the difference between the RMSE values at different lead times is not significant, indicating a lack of sensitivity to the precipitation forecast horizon. However, a modestly increasing trend in RMSE (or loss of skill at longer lead times) is visible in both basins. The uncertainly of the NMME precipitation forecast in Brahmaputra basin is generally lower (<30%) than the Ganges basin (44%–48%; Fig. 5). The ACC trend shows a similar type of assessment for the NMME precipitation forecast (Fig. 6). The pattern of the ACC versus lead time is weakly correlated (<0.35) to lead time. In general, when the ACC values are below 0.6, skill is considered unsatisfactory (Murphy and Epstein 1989).

Next, we performed similar assessment for streamflow forecasting at monthly time scales. The ensembles of forecast hydrograph are shown for both river

locations and for specific lead times (Fig. 7). The reference streamflow (i.e., obtained from SGF data) is found to be bound within the forecast ensembles for most of the period when the flow is lean (November–May). In general, the Ganges River at Hardinge Bridge yields higher variability in forecast (Fig. 7b), while for Brahmaputra (at Bahadurabad), the forecast simulations exhibit higher precision. Forecasts in general are challenged during the late monsoon season (August–October) for the Ganges River (Fig. 7b) and during the monsoon season (June–September) for the Brahmaputra River (Fig. 7a). The precipitation forecast yielded a probabilistic streamflow forecast that also enveloped the reference flow during the rising or receding periods of the highly seasonal flow regimes of the rivers. It should be noted that the spread of the forecast streamflow from all eight ensembles at monthly time scales was very small to yield a
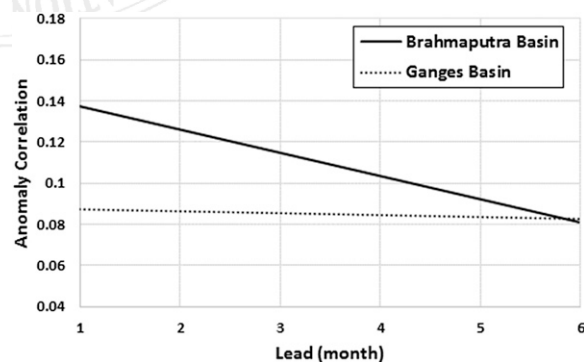
FIG. 6. ACC trend of NMME precipitation forecast (during 1982–2012) as a function of lead time (months) when compared to Princeton global forcing data over the entire Ganges and Brahmaputra basin. Note that the trend is idealized as a linear regression mainly to observe sensitivity to lead time.
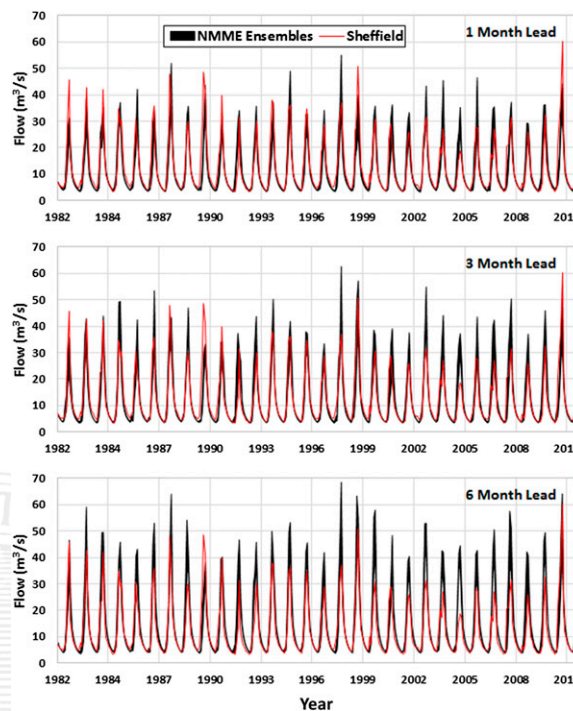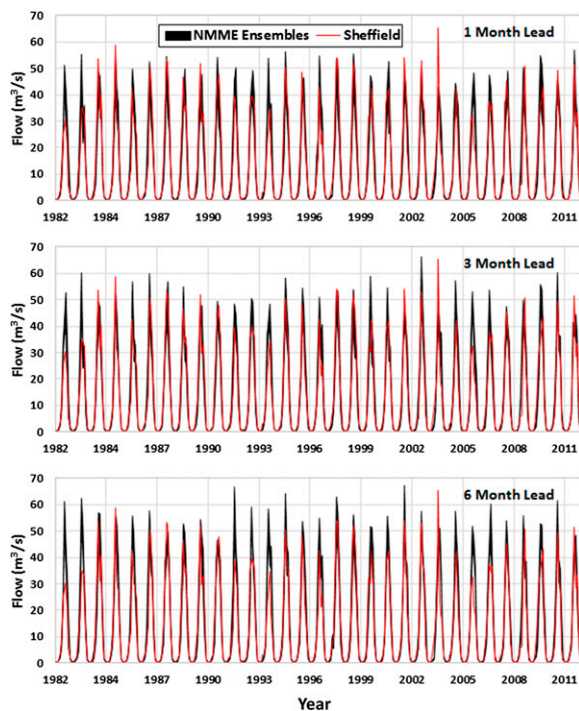
FIG. 7. (a) Monthly average forecast hydrograph showing all eight ensemble members lumped as an envelope of black lines at Bahadurabad (Brahmaputra River). The red line is the hydrograph simulated using SGF. There is no clear distinction in performance in terms of hydrograph spread at increasing lead times. (b) As in (a), but for Hardinge Bridge (Ganges River).

FIG. 7. (*Continued*)

discernible envelope. In terms of relative RMSE (normalized by reference streamflow from SGF; Fig. 8, left), streamflow forecast uncertainty (RMSE) was found to be 38%–50% of the reference flow, with a more consistent trend against lead time compared to precipitation skill (i.e., RMSE rises while ACC decreases reasonably consistently as lead time increases). However, as mentioned earlier, the low ACC observed (<0.35) is indicative of poor skill at the monthly time scale. This indicates that water management based on forecasting at monthly time scales will not be appropriate for the two river basins yet.

The comparison between relative RMSE of the NMME-derived outflow (normalized by in situ observed flow and reference streamflow from SGF) is shown in Fig. 9 to help us understand the combined role of uncertainty due to hydrologic model and downscaling approach based on SGF data. The relative RMSE with respect to the in situ observed flow is almost flat against the lead time, which is inconsistent and points to needed improvements in downscaling using more robust and regionally appropriate forcing datasets and hydrologic model accuracy. The RMSE values normalized by the reference streamflow from SGF are slightly lower than

the in situ RMSE and show a more sensitive trend to lead time. This likely proves that the use of good-quality in situ historical forcings in NMME downscaling may improve the true forecast performance. Again, we do observe that the skill values are quite high (>45%) at monthly time scales, to warrant any useful decision-making.

To explore a more appropriate time scale (than monthly) for the eventual use (operationalization) of streamflow forecast, the seasonal (3-monthly average flow) scale was analyzed. For this purpose, the year was subdivided into four seasons; January–March, April–June, July–September, and October–December. The overall performance of the seasonal analysis is shown in Fig. 10. The relative RMSE that was normalized by reference flow from SGF showed much more sensitivity to lead time (Fig. 10, left). The uncertainty in terms of relative RMSE ranged from 22% to 35% of reference flow at seasonal time scales, which is lower than the uncertainty at monthly time scales. The Brahmaputra basin showed relatively better performance in terms of relative RMSE as well as the ACC (Fig. 10, right). The ACC for Bahadurabad in the Brahmaputra River showed a clear decreasing trend after a 2-month lead. Also, the performance of the Brahmaputra basin significantly increases in the seasonal scale than the monthly scale in both benchmarks (Figs. 8, 10).
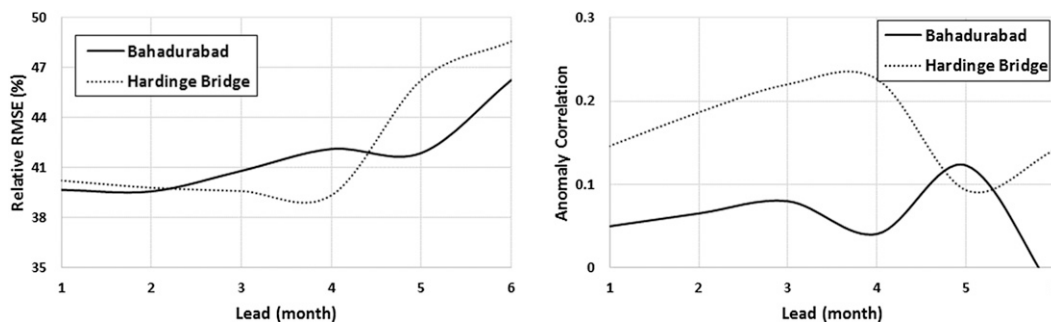
AU22

FIG. 8. (left) Relative RMSE (normalized by the streamflow from SGF) and (right) ACC of the streamflow from NMME average for Brahmaputra at Bahadurabad and Ganges at Hardinge Bridge in monthly scale (1982–2012; 372 months).

F11 F12   Last, Figs. 11 and 12 show the performance of individual seasons with respect to the reference streamflow from SGF in terms of relative RMSE and ACC, respectively. In relative RMSE standards, July–September showed the worst performance (>35%) and January–March showed the best (<10%) for both basins (Fig. 11). But the ACC showed that July–September in the Brahmaputra basin and October–December in the Ganges basin is more skillful than the other seasons (Fig. 12). In both cases, the ACC remained lower than 0.6, even at seasonal time scales.

7. Conclusions

The key features of the study findings can be summarized as follows. In terms of relative RMSE (normalized by reference flow from global forcing), streamflow forecast uncertainty was found to be higher (38%–50%) at monthly time scales and lower (22%–35%) at seasonal time scales. The Ganges River experienced higher uncertainty than the Brahmaputra River in terms of relative RMSE. Skill of the NMME flow forecast in terms of ACC showed similar outcomes, where the seasonal forecast yielded better correlation with the reference flow than the monthly scale. The forecast skill in the Brahmaputra basin showed more improvement in seasonal time scales than the Ganges basin after switching from the monthly scale. Forecast of streamflow during the late monsoon period (August–October) was found to be a little challenging for the lack of NMME precipitation forecast skill during the peak season over the Ganges basin. Overall, the ACC in both monthly and seasonal scales remained well below 0.6.

Earlier we asked whether GCMs are ready to be operationalized for streamflow forecasting in South Asian river basins, and if so, at what temporal scales and water management decisions are they likely to be relevant? Based on the summary of the findings reported

above, which are mostly relative to assuming that reference flow from global forcing is perfectly representative of in situ conditions, our take-home message is that, despite skill improvement of streamflow forecast in seasonal scale for water balance applications, GCMs are not yet ready for prime-time operationalization for a wide variety of multiscale water management decisions for the Ganges and Brahmaputra River basins. In tracing the source of what is likely required to be improved a priori before revisiting these two questions, we have identified the hydrologic model and downscaling approach using a more regionally consistent forcing dataset.

Toward continuous improvement of operational readiness of GCM streamflow forecasting, future studies, in addition to creating better forcings for downscaling and models, need to address the current limitations. A primary hurdle in the way of raising skill of operational forecasting is lack of better hydrologic records and regionally consistent forcing datasets for downscaling across the entire basin (Hossain and Katiyar 200?). Assessment of GCM forecasting as well as hydrologic model improvements should be assessed
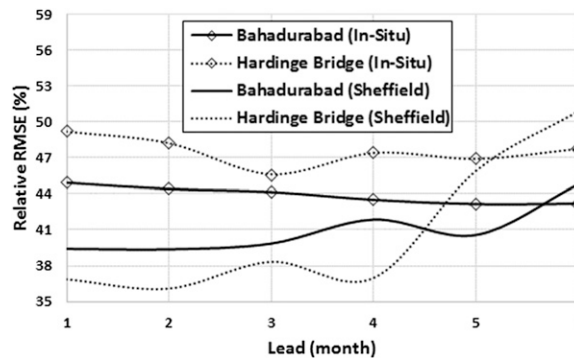
FIG. 9. Relative RMSE of the outflow from NMME average. Normalized by in situ flow and outflow from Princeton forcing (Sheffield) in monthly scale (1985–2010; 312 months).
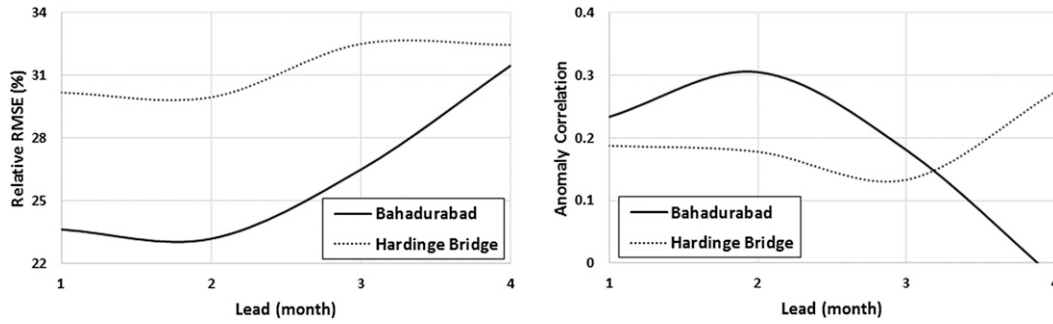
FIG. 10. As in Fig. 8, but for seasonal scale (3-month average of January–March, April–June, July–September, and October–December; 1982–2012; 124 seasons). Note that Brahmaputra yields a slightly more consistent trend with respect to lead time.

at locations that represent smaller drainage areas within the GBM, lower response time (more flashiness), and less seasonality in the flow patterns of flow. For example, the Meghna basin in the northeast suffers from flash flood during spring season. Another issue to address is that of hydromorphology (Vogel 2011) which encompasses the difficult issue of artificial redistribution of surface water by competing upstream parties and cannot be resolved wholly using physical models forced with GCM forecast forcings alone. This is where a satellite-based observational system that routinely monitors the state of surface water (height, surface area, and volume changes) at high space–time resolution and provides clues on water redistribution can potentially be integrated in water forecast modules. Recent work on radar altimeters by Hossain et al. (2013) indicates that the expanding constellation of surface water–relevant satellites may indeed make the monitoring of water management in regulated basins much more feasible. Future assessments of operational readiness of GCMs for seasonal streamflow forecasting in large river systems should therefore also involve the coupling of

water management component assimilating surface water measurements from satellites with a hydrologic model so that the variability due to human activity can be teased out as much as possible.

As noted earlier, the South Asian region is vulnerable to uncertainty in water resources availability that often manifests as shortage (drought or upstream and unilateral extraction by dams or diversion projects), excess (floods), and crop-damaging natural disasters (cyclones and river flooding). Among various options to build resilience against this vulnerability, one of the most cost-effective strategies with a proven benefit-to-cost ratio is to institutionalize a forecasting system that can forecast and warn of the changing dynamics of water cycle parameters (Negri et al. 2005). For example, recent rural household surveys in Bangladesh have revealed that a doubling of the flood forecasting range from 3 to 7 days can potentially minimize losses further from 3% to 20% for the Bangladesh economy (CEGIS 2006). A comprehensive water availability forecasting system during the season when water is limited or in excess can provide routine and early information to beneficiaries such as farmers and water supply managers. For all these
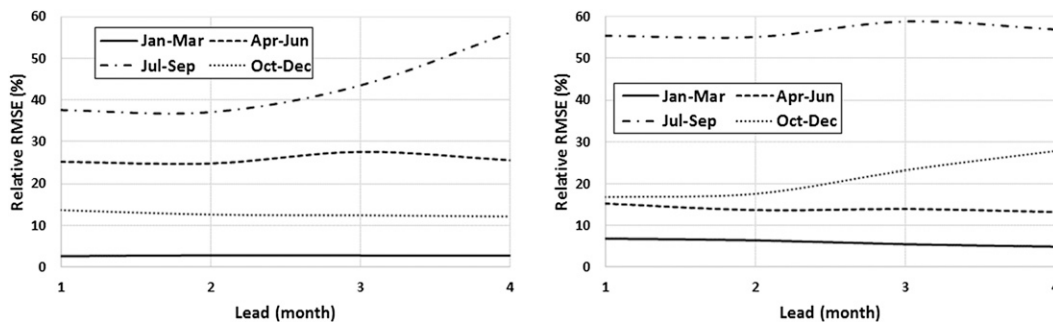
FIG. 11. Relative RMSE of the streamflow from NMME average (normalized by the streamflow from SGF) at seasonal time scales for different seasons (1982–2012, ~~31 data/seasons~~): (left) Bahadurabad in the Brahmaputra River and (right) Hardinge Bridge in the Ganges River.
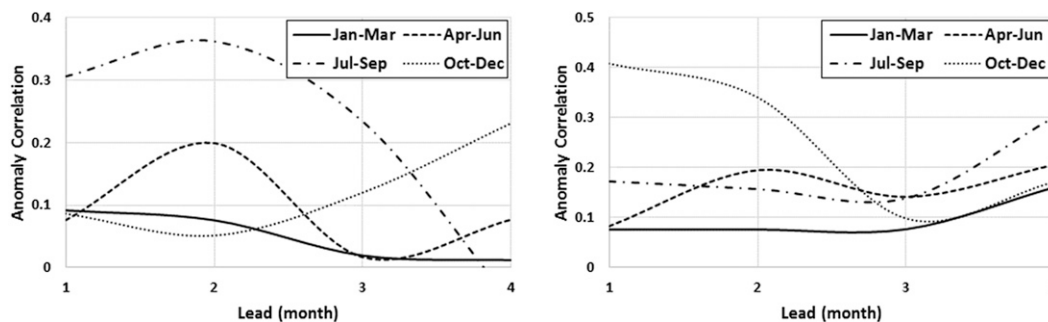
FIG. 12. ACC of NMME forecast with streamflow from SGF at seasonal time scales for different seasons (1982–2012; 30 seasons): (left) Bahadurabad in the Brahmaputra River and (right) Hardinge Bridge in the Ganges River.

reasons, the systematic improvement of the downscaling procedure using regionally consistent historical forcings and improved hydrologic models should be a high priority to make better use of gradually improving GCMs in the future. When GCMs are ready for operationalization, water balance–based management decisions at seasonal time scales should be practiced before pushing the envelope toward monthly time scales, which seems quite impossible according to our study given the current state of the art.

REFERENCES

Adler, R. F., and Coauthors, 2003: The version 2 Global Precipitation Climatology Project (GPCP) monthly precipitation analysis (1979–present). *J. Hydrometeor.*, **4**, 1147–1167, doi:10.1175/1525-7541(2003)004<1147:TVGPCP>2.0.CO;2.

Alexander, M. A., I. Bladé, M. Newman, J. R. Lanzante, N. C. Lau, and J. D. Scott, 2002: The atmospheric bridge: The influence of ENSO teleconnections on air–sea interaction over the global oceans. *J. Climate*, **15**, 2205–2231, doi:10.1175/1520-0442(2002)015<2205:TABTIO>2.0.CO;2.

Becker, E. J., H. van den Dool, and M. Peña, 2013: Short-term climate extremes: Prediction skill and predictability. *J. Climate*, **26**, 512–531, doi:10.1175/JCLI-D-12-00177.1.

Byerlee, D., 1992: Technical change, productivity, and sustainability in irrigated cropping systems of South Asia: Emerging issues in the post-green revolution era. *J. Int. Dev.*, **4**, 477–496, doi:10.1002/jid.3380040502.

CEGIS, 2006: Sustainable end-to-end climate/flood forecast application through pilot projects showing measurable improvements. CEGIS Rep., 78 pp. [Available online http://www.cegisbd.com/report.html]   **AU11**

Chowdhury, M. R., and N. Ward, 2004: Hydro-meteorological variability in the greater Ganges–Brahmaputra–Meghna basins. *Int. J. Climatol.*, **24**, 1495–1508, doi:10.1002/joc.1076.

Costa-Cabral, M. C., J. E. Richey, G. Goteti, D. P. Lettenmaier, and C. Feldkötter, 2008: Landscape structure and use, climate, and water movement in the Mekong River basin. *Hydrol. Processes*, **22**, 1731–1746, doi:10.1002/hyp.6740.

Dyurgerov, M. B., and M. F. Meier, 2005: Glaciers and the changing earth system: A 2004 snapshot. Occasional Paper No. 58, INSTAAR, University of Colorado, 116 pp. [Available online at http://instaar.colorado.edu/uploads/occasional-papers/OP58_dyurgerov_meier.pdf.]

Funk, C., and J. Michaelsen, 2004: A simplified diagnostic model of orographic rainfall for enhancing satellite-based rainfall estimates in data-poor regions. *J. Appl. Meteor.*, **43**, 1366–1378, doi:10.1175/JAM2138.1.   **AU12**

——, A. Hoell, S. Shukla, I. Bladé, B. Liebmann, J. B. Roberts, F. R. Robertson, and G. Husak, 2014: Predicting East African spring droughts using Pacific and Indian Ocean sea surface temperature indices. *Hydrol. Earth Syst. Sci.*, **18**, 4965–4978, doi:10.5194/hess-18-4965-2014.   **AU13**

Hagedorn, R., F. Doblas-Reyes, and T. Palmer, 2005: The rationale behind the success of multi-model ensembles in seasonal forecasting—I. Basic concept. *Tellus*, **57A**, 219–233, doi:10.1111/j.1600-0870.2005.00103.x.

Hamlet, A. F., and D. P. Lettenmaier, 1999a: Effects of climate change on hydrology and water resources in the Columbia River basin. *J. Amer. Water Resour. Assoc.*, **35**, 1597–1623, doi:10.1111/j.1752-1688.1999.tb04240.x.

——, and ——, 1999b: Columbia River streamflow forecasting based on ENSO and PDO climate signals. *J. Water Resour. Plann. Manage.*, **125**, 333–341, doi:10.1061/(ASCE)0733-9496(1999)125:6(333).

Ho, C. K., D. B. Stephenson, M. Collins, C. T. Ferro, and S. J. Brown, 2012: Calibration strategies: A source of additional

~~uncertainty in climate change projections.~~ *~~Bull. Amer. Meteor.~~* *~~Soc.~~*, ~~93, 21–26, doi:10.1175/2011BAMS3110.1.~~

Hopson, T. M., and P. J. Webster, 2010: A 1–10 day ensemble forecasting scheme for the major river basins of Bangladesh: Forecasting severe floods of 2003–07. *J. Hydrometeor.*, **11**, 618–641, doi:10.1175/2009JHM1006.1.

Hossain, F., 2014: Paradox of Peak Flows in a Changing Climate. *J. Hydrol. Eng.*, 19, 02514001, doi:10.1061/(ASCE)HE.1943-5584.0001059.

——, and N. Katiyar, 2006: Improving flood forecasting in international river basins. *Eos, Trans. Amer. Geophys. Union*, **87** (5), 49–50, doi:10.1029/2006EO050001.

——, A. H. Siddique-E-Akbor, L. C. Mazumder, S. M. ShahNewaz, S. Biancamaria, H. Lee, and C. K. Shum, 2013: Proof of concept of an altimeter-based river forecasting system for transboundary flow inside Bangladesh. *IEEE J. Sel. Top. Appl. Remote Sens.*, **7**, 587–601, doi:10.1109/JSTARS.2013.2283402.

——, and Coauthors, 2014: Crossing the ''Valley of Death'': Lessons learned from implementing an operational satellite-based flood forecasting system. *Bull. Amer. Meteor. Soc.*, **95**, 1201–1207, doi:10.1175/BAMS-D-13-00176.1.

IPCC, 2013: What is a GCM? Data Distribution Centre, IPCC, accessed 13 March 2014. [Available online at http://www.ipcc-data.org/guidelines/pages/gcm_guide.html.]

Kirtman, B. P., and Coauthors, 2014: The North American Multimodel Ensemble: Phase-1 seasonal-to-interannual prediction; Phase-2 toward developing intraseasonal prediction. *Bull. Amer. Meteor. Soc.*, **95**, 585–601, doi:10.1175/BAMS-D-12-00050.1.

Klein, S. A., B. J. Soden, and N.-C. Lau, 1999: Remote sea surface temperature variations during ENSO: Evidence for a tropical atmospheric bridge. *J. Climate*, **12**, 917–932, doi:10.1175/1520-0442(1999)012<0917:RSSTVD>2.0.CO;2.

Kundzewicz, Z. W., and E. Z. Stakhiv, 2010: Are climate models ''ready for prime time'' in water resources management applications, or is more research needed? *Hydrol. Sci. J.*, **55**, 1085–1089, doi:10.1080/02626667.2010.513211.

Liang, X., D. P. Lettenmaier, E. F. Wood, and S. J. Burges. 1994: A simple hydrologically based model of land surface water and energy fluxes for general circulation models. *J. Geophys. Res.*, **99**, 14 415–14 428, doi:10.1029/94JD00483.

Lohmann, D., E. Raschke, B. Nijssen, and D. P. Lettenmaier, 1998: Regional scale hydrology: I. Formulation of the VIC-2L model coupled to a routing model. *Hydrol. Sci. J.*, **43**, 131–141, doi:10.1080/02626669809492107.

Mirza, M. Q. M., 1998: Diversion of the Ganges water at Farakka and its effects on salinity in Bangladesh. *Environ. Manage.*, **22**, 711–722, doi:10.1007/s002679900141.

Misra, A. K., A. Saxena, M. Yaduvanshi, A. Mishra, Y. Bhauduriya, and A. Takur, 2007: Proposed river linking project of India: Boon or bane to nature? *Environ. Geol.*, **51**, 1361–1376, doi:10.1007/s00254-006-0434-7.

Miyakoda, K., G. D. Hembree, R. F. Strickler, and I. Shulman, 1972: Cumulative results of extended forecast experiments: I. Model performance for winter cases. *Mon. Wea. Rev.*, **100**, 836–855, doi:10.1175/1520-0493(1972)100<0836:CROEFE>2.3.CO;2.

Müller, W. A., C. Appenzeller, F. J. Doblas-Reyes, and M. A. Liniger, 2005: A debiased ranked probability skill score to evaluate probabilistic ensemble forecasts with small ensemble sizes. *J. Climate*, **18**, 1513–1523, doi:10.1175/JCLI3361.1.

Murphy, A. H., and E. S. Epstein, 1989: Skill scores and correlation coefficients in model verification. *Mon. Wea. Rev.*, **117**, 572–582, doi:10.1175/1520-0493(1989)117<0572:SSACCI>2.0.CO;2.

Negri, A. J., and Coauthors, 2005: The hurricane–flood–landslide continuum. *Bull. Amer. Meteor. Soc.*, **86**, 1241–1247, doi:10.1175/BAMS-86-9-1241.

Nishat, A., and I. M. Faisal, 2000: An assessment of the institutional mechanisms for water negotiations in the Ganges–Brahmaputra–Meghna system. *Int. Negot.*, **5**, 289–310, doi:10.1163/15718060020848776.

Nishat, B., and M. Rahman, 2009: Water resources modeling of the Ganges–Brahmaputra–Meghna River basins using satellite remote sensing data. *J. Amer. Water Resour. Assoc.*, **45**, 1313–1327, doi:10.1111/j.1752-1688.2009.00374.x.

NRC, 2010: *Assessment of Intraseasonal to Interannual Climate Prediction and Predictability*. National Academies Press, 192 pp.

Pielke, R. A., Sr., 1998: Climate prediction as an initial value problem. *Bull. Amer. Meteor. Soc.*, **79** (12), 2743–2745.

Reynolds, R. W., T. M. Smith, C. Liu, D. B. Chelton, K. S. Casey, and M. G. Schlax, 2007: Daily high-resolution-blended analyses for sea surface temperature. *J. Climate*, **20**, 5473–5496, doi:10.1175/2007JCLI1824.1.

Salas, J. D., B. Rajagopalan, L. Saito, and C. Brown, 2012: Special section on climate change and water resources: Climate nonstationarity and water resources management. *J. Water Resour. Plann. Manage.*, **138**, 385–388, doi:10.1061/(ASCE)WR.1943-5452.0000279.

Shah, R. B., 2001: Ganges–Brahmaputra: The outlook for the twenty-first century. *Sustainable Development of the Ganges–Brahmaputra–Meghna Basins*, A. K. Biswas and J. I. Uitto, eds., Oxford University Press, 17–45.

Sheffield, J., G. Goteti, and E. F. Wood, 2006: Development of a 50-year high-resolution global dataset of meteorological forcings for land surface modeling. *J. Climate*, **19**, 3088–3111, doi:10.1175/JCLI3790.1.

——, B. Livneh, and E. F. Wood, 2012: Representation of terrestrial hydrology and large-scale drought of the continental United States from the North American Regional Reanalysis. *J. Hydrometeor.*, **13**, 856–876, doi:10.1175/JHM-D-11-065.1.

Shrestha, K. Y., P. J. Webster, and V. E. Toma, 2014: An atmospheric–hydrologic forecasting scheme for the Indus River basin. *J. Hydrometeor.*, **15**, 861–890, doi:10.1175/JHM-D-13-051.1.

Siddique-E-Akbor, A. H. M., F. Hossain, S. Sikder, C. K. Shum, S. Tseng, Y. Yi, F. J. Turk, and A. Limaye, 2014: Satellite precipitation data–driven hydrological modeling for water resources management in the Ganges, Brahmaputra, and Meghna basins. *Earth Interact.*, 18, doi:10.1175/EI-D-14-0017.1.

Sikder, S., and F. Hossain, 2014: Understanding the geophysical sources of uncertainty for Satellite Interferometric (SRTM)-based discharge estimation in river deltas: The case for Bangladesh. *IEEE J. Sel. Top. Appl. Earth Obs. Remote Sens.*, **8**, 523–538, doi:10.1109/JSTARS.2014.2326893.

Sinha, I. N., 1995: Opportunity, delay and policy planning vision in the synergic development of eastern Himalayan rivers: A conspectus. *Int. J. Water Resour. Dev.*, **11**, 303–314, doi:10.1080/07900629550042254.

Vogel, R. M., 2011: Hydromorphology. *J. Water Resour. Plann. Manage.*, **137**, 147–149, doi:10.1061/(ASCE)WR.1943-5452.0000122.

AU14

AU15

AU16

Webster, P. J., 2013: Improve weather forecasts for the developing world. *Nature*, **493**, 17–19, doi:10.1038/493017a.

Wilby, R. L., T. M. L. Wigley, D. Conway, P. D. Jones, B. C. Hewitson, J. Main, and D. S. Wilks, 1998: Statistical downscaling of general circulation model output: A comparison of methods. *Water Resour. Res.*, **34**, 2995–3008, doi:10.1029/98WR02577.

Wilks, D. S., 2011: *Statistical Methods in the Atmospheric Sciences*. 3rd ed., International Geophysics Series, Vol. 100, Academic Press, 704 pp.

Wood, A. W., E. P. Maurer, A. Kumar, and D. P. Lettenmaier, 2002: Long-range experimental hydrologic forecasting for the eastern United States. *J. Geophys. Res.*, **107**, 4429, doi:10.1029/2001JD000659.

Wu, H., R. F. Adler, Y. Hong, Y. Tian, and F. Policelli, 2012: Evaluation of global flood detection using satellite-based rainfall and a hydrologic model. *J. Hydrometeor.*, **13**, 1268–1284, doi:10.1175/JHM-D-11-087.1.

Xie, P., A. Yatagai, M. Chen, T. Hayasaka, Y. Fukushima, C. Liu, and S. Yang, 2007: A gauge-based analysis of daily precipitation over East Asia. *J. Hydrometeor.*, **8**, 607–627, doi:10.1175/JHM583.1.

Yatagai, A., K. Kamiguchi, O. Arakawa, A. Hamada, N. Yasutomi, and A. Kitoh, 2012: APHRODITE: Constructing a long-term daily gridded precipitation dataset for Asia based on a dense network of rain gauges. *Bull. Amer. Meteor. Soc.*, **93**, 1401–1415, doi:10.1175/BAMS-D-11-00122.1.

Yuan, X., E. F. Wood, and Z. Ma. 2015: A review on climate-model-based seasonal hydrologic forecasting: physical understanding and system development. *Wiley Interdiscip. Rev.: Water*, **2**, 523–536, doi:10.1002/wat2.1088.

AU17

AU18